

Quantitative Susceptibility Mapping of Lesions in Multiple Sclerosis

Ahmed M. Elkady¹, Hongfu Sun¹, Andrew J. Walsh¹, Gregg Blevins², Zhuozhi Dai¹, and Alan H. Wilman¹

¹Dept. of Biomedical Engineering, University of Alberta, Edmonton, AB, Canada. ²Division of Neurology, University of Alberta, Edmonton, AB, Canada

Introduction: Quantitative Susceptibility Mapping (QSM) is a new method that has evolved from phase imaging, and provides a means to examine myelin and iron content of lesions in Multiple Sclerosis (MS) [1,2]. This may provide additional valuable information beyond standard T2 and T1-weighted MRI used in the clinic. We examine QSM and phase imaging [3-6], in addition to a quantitative relaxation method, R2*, to study MS lesion shape and conspicuity in comparison to conventional T2 and T1-weighted MRI using both *in vivo* and *post mortem* subjects. While QSM offers true information on MS lesion shape and contrast, phase imaging is hampered by non-local effects [1]. However, phase may provide an estimate of iron presence in lesions by examining for dipole field patterns [7] (Fig. 1), which may not be possible using susceptibility (SUS) alone due to confounding effects of myelin loss [8].

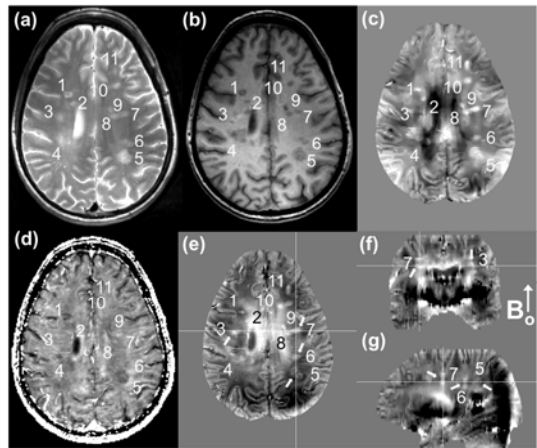


Figure 2 Example images from a RRMS subject. T2-weighted (a), T1-weighted (b), SUS (c), R2* (d), and axial LFS (e), coronal LFS (f), and sagittal LFS (g) showing 11 MS lesions. Hyper/iso contrast for center/ring is apparent in all lesions in SUS (2c), except for lesion 5 which shows hyper/hyper. The majority of lesions are not visible in R2* (2d), but they are visible in LFS (2e). Corresponding LFS coronal and sagittal (2f,g) slices confirmed dipole patterns for lesions 6 and 7, which agree to the displayed hypo-ring for lesion 7 (2e), and lesion 6 in a nearby slice (not displayed).

axial slices and stained with Perls' iron stain to identify iron in MS lesions, with only 8 lesions with a complete stain, and fourteen with no stain out of a total of 22 lesions [11].

Results: Table 1 demonstrates lesion core/ring contrast as a percentage of the total 351 lesions identified, while Table 2 shows the lesion contrast compared to the Perl's iron stain status for 22 lesions identified by pathology in 2 postmortem patients. Fig. 2 shows one slice from an RRMS subject identifying 11 MS lesions from T2- and T1-weighted MRI (2a,b). Fig. 3 displays the only lesion positively stained for Perl's staining that showed a dipole pattern in LFS maps and core hyper-intensity in QSM.

Discussion: SUS lesion contrast is regulated by changes in iron and myelin; increased iron presence causes an increase in susceptibility due to the paramagnetic nature of iron, in contrast to diamagnetic myelin, which causes increased susceptibility upon demyelination. Conversely, R2* increases with iron gain and decreases with myelin loss. Thus, SUS and R2* offer complementary information that enable delineation of the origin of susceptibility contrast [12]. Our findings indicate that hyper and hypo-intensive lesion core (Table 1) are the dominant contrast in SUS and R2*, respectively. This suggests that demyelination is the dominant contrast contributor in MS lesions, which is in agreement with previous similar work [2]. The small percentage of dipoles observed herein (12%) also confirms this observation, which is on the order of the number of dipoles observed by others (4%) [7]. However, we suggest that dipole patterns in LFS could affirm the presence of iron (Fig. 3), but could not be used to conclude iron absence because the majority (7 out of 8) of iron-positive lesions did not demonstrate dipoles. The rare conspicuity of iron-positive lesions with dipoles in LFS MRI can be attributed to the dominance of other contrast contributors in the vicinity of the lesion, which can impair dipole identification. The majority of positive iron stained lesions (Table 2) was visible on LFS and SUS maps as a hyper-core with no ring, but a large percentage also presented as iso-core in LFS with or without a hypo-ring. None-stained lesions rarely exhibited rings in either LFS and SUS maps, and mostly exhibited iso-core contrast in SUS.

Conclusion: The majority of MS lesions present *in vivo* as hyper-core without a ring in LFS and SUS maps, while showing as hypo-core without a ring in R2*, which verifies that demyelination is the dominant contrast mechanism in these lesions. Iron-stained postmortem MS lesions indicate that dipole patterns in LFS and hyper-core contrast in LFS or SUS could be used for confirmation of iron presence, but could not be used to rule out the presence of iron.

References: [1] Eskreis-Winkler 2014, J Magn Res Imaging; [2] Li 2014, ISMRM #0895; [3] Yao 2012, Radiology, 262:206; [4] Hammond 2008, Ann Neurol 64(6):707; [5] Haacke 2009, J Magn Res Imaging, 29(3):537; [6] Mehta 2013, PLoS One, 8(3):e57573; [7] Wiggermann 2014, ISMRM #0894; [8] Wisniewski 2014, MRM Epub; [9] Sun 2014, MRM 71:1151; [10] Wu 2012, MRM 67:137; [11] Walsh 2014, Radiology, 270:186, [12] Deistung 2012, Neuroimage 65:299.

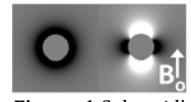


Figure 1 Spheroid's dipole field in axial phase (left) & sagittal/coronal (right).

Materials & Methods: *In Vivo:* Twenty clinically confirmed relapsing-

remitting MS subjects (4/16 M/F, 33.5 ± 8.3 years) who underwent examination using 4.7T MRI were retrospectively selected. Hyperintensity on T2-weighted FSE and FLAIR, and hypo-intensity on non-enhanced T1-weighted mp-RAGE were used to define 351 MS lesions, with validation by a radiologist. QSM was performed after phase unwrapping, brain extraction, background field removal [9], and inversion of the phase data [10]. Dipole field patterns (Fig. 1), and hypo, hyper, iso, or heterogeneous contrast of the core/ring of lesions relative to surrounding normal appearing white matter were visually evaluated in $R2^* = 1/T2^*$, SUS and Local Field Shift (LFS = $-\frac{\varphi_{local}}{y \cdot TE \cdot B_0}$). All acquisitions were manually

registered and interpolated to a resolution of $0.38 \times 0.38 \times 2$ mm.

Post Mortem: *In situ* MR imaging hours after death was performed on two secondary progressive MS subjects. MRI protocols and image processing were similar to the *in vivo* study, but the images were interpolated to an isotropic resolution of 0.25 mm to better compare to pathology images. Pathology examination was performed using 8-mm



Figure 3 Iron-laden lesion with Perls' staining in pathology section (left), and corresponding *in-situ* axial QSM with hyper-contrast and no ring (mid-left). Corresponding axial, sagittal and coronal LFS (right) showing a dipole pattern with yellow crosshairs through center in each view.

Table 1 Center/ring contrast of MS lesions as a % of the total 351 identified lesions.

	SUS.	LFS	R2*
Center / Ring Contrast (%)	(%)	(%)	(%)
iso / iso (Not Visible)	46.3	40.3	30.1
hypo / hypo	0.0	0.0	1.8
hyper / hyper	0.9	1.0	0.0
hypo / hyper	2.6	1.5	4.3
hypo / iso	3.2	8.7	52.2
hyper / hypo	6.4	0.9	1.1
hyper / iso	26.9	40.8	7.0
hetero / hyper	1.4	0.4	0.2
hetero / hypo	0.6	0.0	0.2
hetero / iso	1.8	2.3	0.0
iso / hyper	6.2	2.6	2.1
iso / hypo	3.7	1.5	1.2
Dipole (% of visible)	n/a	12.4	n/a

Table 2 Center/ring contrast of MS lesions and corresponding Perl's iron stain status as a % of total of 22 lesions in 2 postmortem patients.

Iron Stain	Center Contrast (% of Total)			Ring Contrast (% of Total)		
	LFS		SUS	LFS		SUS
	hypo	hyper	iso	hypo	hyper	iso
Complete	0	18	14	5	5	27
None	5	36	23	0	14	36
				14	0	23
				5	32	0
				0	9	55
				0	0	64